Supplement of Atmos. Chem. Phys., 15, 5211–5228, 2015
http://www.atmos-chem-phys.net/15/5211/2015/
doi:10.5194/acp-15-5211-2015-supplement

Atmospheric Chemistry and Physics
Open Access

Supplement of

Fine-particle water and pH in the southeastern United States

H. Guo et al.

Correspondence to: R. J. Weber (rodney.weber@eas.gatech.edu) and A. Nenes (athanasios.nenes@gatech.edu)

Supplementary materials

1. Nephelometer RH sensor calibration

The nephelometer RH sensors were calibrated by placing the sensors in a sealed container above aqueous saturated salt solutions at known temperatures for an accurate prediction of equilibrium RH (Greenspan, 1977). More than 3hrs were allowed for each salt solution to reach water vapor saturation.

Table. S1. Theoretical and measured RH for saturated salt solution at 20℃

Compound	Equilibrium RH, %	Measured RH, %
K_2CO_3	43.16 ±0.33	40.39 ±0.47
NaCl	75.47 ±0.14	71.00 ±0.00
KCl	85.11 ±0.29	80.21 ±0.38
KNO_3	94.62 ±0.66	88.60 ±0.47

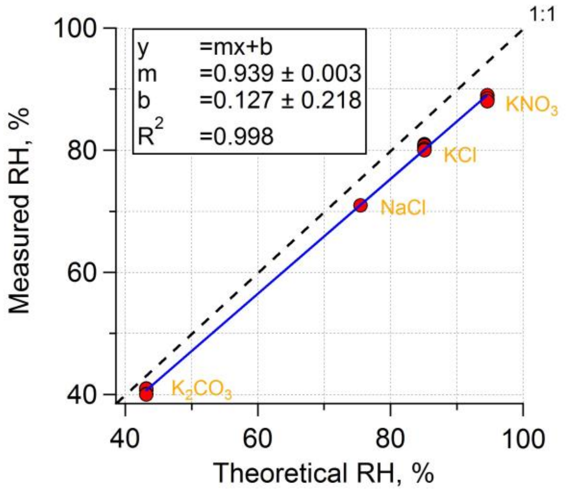

Fig. S1. A linear regression fit of measured RH.

2. LWC measurement principle by nephelometers

Particle water was indirectly measured by two nephelometers. The difference between ambient and dry scattering coefficients (σ_{sp}) is assumed to be caused by the loss of water. The ratio between ambient scattering coefficient and dry scattering coefficient is referred to as $f(RH)$.

$$f(RH) = \frac{\sigma_{sp}(ambient)}{\sigma_{sp}(dry)} = \frac{\int \frac{\pi}{4} Q_{s,ambient} D_{p,ambient}{}^{2} N(D_p) dD_p}{\int \frac{\pi}{4} Q_{s,dry} D_{p,dry}{}^{2} N(D_p) dD_p} \tag{1}$$

where $Q_{s,ambient}$ and $Q_{s,dry}$ are scattering efficiencies in ambient and dry conditions, respectively. $N(D_p)$ is the particle number distribution function. If N_t is the total number concentration, and $\overline{D_p}$ is the diameter of average surface, and $\overline{Q_{s,ambient}}$ and $\overline{Q_{s,dry}}$ are average scattering efficiencies, then,

$$\frac{\sigma_{sp}(ambient)}{\sigma_{sp}(dry)} = \frac{\frac{\pi}{4}\overline{Q_{s,ambient}}\,\overline{D_{p,ambient}}^{2} N_t}{\frac{\pi}{4}\overline{Q_{s,dry}}\,\overline{D_{p,dry}}^{2} N_t} = \frac{\overline{Q_{s,ambient}}\,\overline{D_{p,ambient}}^{2}}{\overline{Q_{s,dry}}\,\overline{D_{p,dry}}^{2}} \tag{2}$$

$$\overline{D_{p,ambient}} = \overline{D_{p,dry}}\sqrt{f(RH)\,\overline{Q_{s,dry}}/\overline{Q_{s,ambient}}} \tag{3}$$

We assume:

$$\frac{\overline{Q_{s,ambient}}}{\overline{Q_{s,dry}}} \approx 1 \tag{1}$$

Combining Eq. 3 and Eq. 4 we get,

$$\overline{D_{p,ambient}} = \overline{D_{p,dry}}\sqrt{f(RH)} \tag{5}$$

LWC is then equal to the differences between ambient particle volume and dry particle volume.

$$LWC = \left(\frac{\pi}{6}\overline{D_{p,ambient}}^{3} N_t - \frac{\pi}{6}\overline{D_{p,dry}}^{3} N_t\right)\rho_w \tag{6}$$

where ρ_w is water density (constant 1 g cm^{-3} is applied). Furthermore,

$$\overline{D_{p,dry}}^{3} = \frac{m_p}{\frac{\pi}{6}\rho_p N_t} \tag{7}$$

where m_p is dry $PM_{2.5}$ mass concentration and ρ_p is the density of dry aerosol. For SOAS, dry $PM_{2.5}$ mass concentrations were measured by a TEOM (tapered element oscillating microbalance, 1400a, Thermo Fisher Scientific Inc., operated by Atmospheric Research & Analysis Inc.). Combining Eq. 5, Eq. 6, and Eq. 7 gives

$$f(RH)\_water = [f(RH)^{1.5} - 1]m_p\rho_w/\rho_p \tag{8}$$

where $f(RH)$_water refers to the particle water calculated by the above method. ρ_p was estimated from the particle composition including AMS total organics, ammonium, and sulfate, which accounted for 90% of the measure $PM_{2.5}$ dry mass (TEOM) based on the SOAS study average. A typical organic density 1.4 g cm^{-3} is assumed (Turpin and Lim, 2001; King et al., 2007; Engelhart et al., 2008; Kuwata et al., 2012; Cerully et al., 2014), and the density of ammonium sulfate is assumed to be 1.77 g cm^{-3} (Sloane et al., 1991; Stein et al., 1994). ρ_p is calculated to be 1.49 ± 0.04 g cm^{-3} (n = 4,393) using the following relation.

$$\rho_p = \frac{1}{\varepsilon(NH_4^+ + SO_4)/1.77 + \varepsilon(Organics)/1.4} \tag{9}$$

where $\varepsilon(x)$ is the mass fraction of the species x in the aerosol, and ρ_p is the particle density in $g\ cm^{-3}$. The diurnal variation of aerosol dry density is shown in Figure S2.

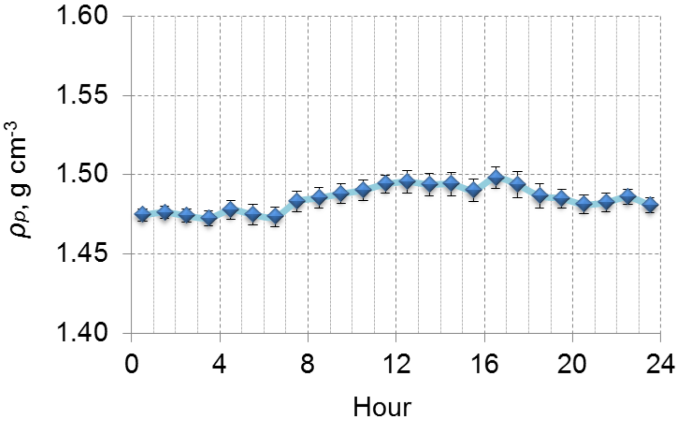

Fig. S2. Predicted PM$_{2.5}$ dry density diurnal profile. Median hourly density averages and SE bars at local hour are plotted.

Eq.4 is a simplifying assumption that introduces error in the calculated LWC. To quantify this, we first need to determine the actual $\overline{Q_{s,ambient}}/\overline{Q_{s,dry}}$ and from the relationship of liquid water, $f(RH)$ and scattering efficiency

$$LWC = \left\{\left[\frac{f(RH)}{\overline{Q_{s,ambient}}/\overline{Q_{s,dry}}}\right]^{1.5} - 1\right\} m_p \rho_w / \rho_p \tag{10}$$

we can estimate the LWC error associated with using Eq.4 in place of the actual $\overline{Q_{s,ambient}}/\overline{Q_{s,dry}}$. To determine the actual $\overline{Q_{s,ambient}}/\overline{Q_{s,dry}}$, we need to compute the scattering efficiency for the dry and humidified particles. For this, we need to determine the dry and wet particle size distributions and their corresponding refractive indices. Dry size distributions are obtained from in-situ measurements (Nguyen et al., 2014), while the corresponding humidified distributions were calculated for predetermined values of the particle diameter-based growth factor, $gf_D = D_{p,wet}/D_{p,dry}$, applied to the dry distribution. The mass composition of wet and dry aerosol is related to gf_D as follows:

$$gf_D = \sqrt[3]{(m_{p,wet}/\rho_{p,wet}) \big/ (m_p/\rho_p)} \tag{11}$$

where $m_{p,wet}$ and $\rho_{p,wet}$ are particle mass concentration and density at humidified (i.e., dry aerosol + water) condition, respectively. From observations of particle dry mass (i.e. TEOM) and the liquid water content calculation outlined in the main text, we can obtain values of gf_D as a function of RH (Fig. S3). In SOAS, the observed campaign-average gf_D = 1.24 ± 0.15.

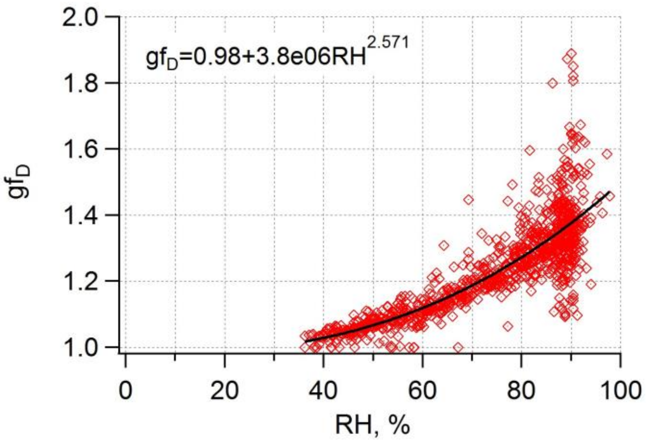

Fig. S3. gf_D plotted as a function of ambient RH based on the SOAS data set.

The particle refractive index (m_r) for wet and dry aerosol is determined as the volume-average ($\overline{m_r}$) of the refractive indices of all aerosol components (Seinfeld and Pandis, 2006),

$$\overline{m_r} = \sum_{i=1}^{n} m_{r,i} f_i \tag{12}$$

where $m_{r,i}$ is the refractive index of component i, and f_i is its volume fraction, and n is the number of constituents (including water) contained in the aerosol. The refractive indices of four major aerosol constituents in SOAS aerosol are listed in Table S2 (NH_4^+/SO_4^{2-} molar ratio was 1.4 ±0.5, so NH_4HSO_4 was assumed to be the dominant form of ammonium and sulfate). f_i was calculated based on the mean mass loadings with or without LWC. LWC was computed from the particle dry mass and diameter-based growth factor (gf_D).

$$m_w = \frac{m_p \rho_w}{\rho_p}\left(gf_D^3 - 1\right) \tag{13}$$

where m_w, ρ_w are LWC mass concentration and density, respectively; m_p, ρ_p are the dry $PM_{2.5}$ mass and density, respectively. From the above, we obtain m_r = 1.539 – 0.023i (gf_D = 1, i.e. dry particle), m_r = 1.488 – 0.017i (gf_D = 1.1), m_r = 1.452 – 0.013i (gf_D = 1.2), m_r = 1.441 – 0.012i (gf_D = 1.24), m_r = 1.427 – 0.010i (gf_D = 1.3), and m_r = 1.408 – 0.008i (gf_D = 1.4).

Table. S2. Refractive indices ($m_r = n + ik$), densities, and mass loadings of particle components.

Substance	n	k	ρ, g cm^{-3}	mean concentration, µg m^{-3}	m_r source
H_2O	1.333	0	1.0	4.50	(Seinfeld and Pandis, 2006)
NH_4HSO_4	1.473	0	1.77	2.19	(Seinfeld and Pandis, 2006)
Organics	1.55	0	1.4	3.32	(Stelson, 1990; Hand and Kreidenweis, 2002)
Black carbon	1.96	-0.66	2	0.26	(Stelson, 1990)

Note: m_{r,H_2O} and m_{r,NH_4HSO_4} refer to the refractive indices at λ = 589nm.

The size distributions and the refractive indices calculated as a function of gf_D are then introduced into Mie Theory (Wiscombe, 1980; Graaff et al., 1992) and subsequently integrated over the dry and humidified size distributions via the MiePlot Version 4.4 (http://www.philiplaven.com/mieplot.htm) software (Laven, 2013) to determine the respective scattering efficiencies. The light scattering calculations are carried out based on a single wavelength (λ = 530nm) at which the nephelometer operates and assuming a temperature at the SOAS-average value of 24.7 ℃.

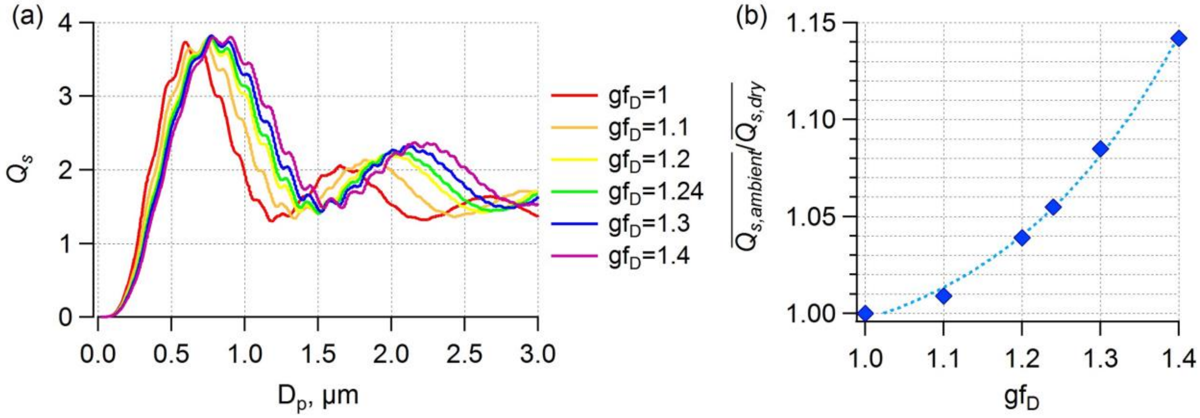

Fig. S4. (a) A single spherical particle scattering efficiency (Q_s) over $PM_{2.5}$ size range at λ = 530 nm; (b) Q_s ratio ($\overline{Q_{s,ambient}}/\overline{Q_{s,dry}}$) plotted versus gf_D for the average SOAS dry size distribution reported by Nguyen et al. (2014).

On average, we find that the actual $\overline{Q_{s,ambient}}/\overline{Q_{s,dry}}$ =1.06, associated with the average SOAS gf_D of 1.24 (Fig. S4b). From the correlations between RH and gf_D (Fig. S3) and between $\overline{Q_{s,ambient}}/\overline{Q_{s,dry}}$

with gf_D (Fig. S4b), we can then apply Eq. 10 to determine the LWC. $f(RH)$_water is then compared against LWC (Fig. S5) to quantify the LWC bias associated with application of Eq. 4. From the above, the LWC error is 10% at gf_D = 1.24 (RH = 76.4%), but approaches 21% at RH = 90% (Fig. S6). Note that the particle dry size distributions from Nguyen et al. (2014) ranged from 6nm to 1 µm. The particles in the size range between 1 µm and 2.5 µm also contribute to particle scattering (as found by Bergin et al. (2001), but may be negligible in this case, since 90% PM$_{2.5}$ mass was found in PM$_1$) and make $\overline{Q_{s,ambient}}/\overline{Q_{s,dry}}$ closer to 1, because they have similar Q_s, as shown in Fig. S4a).

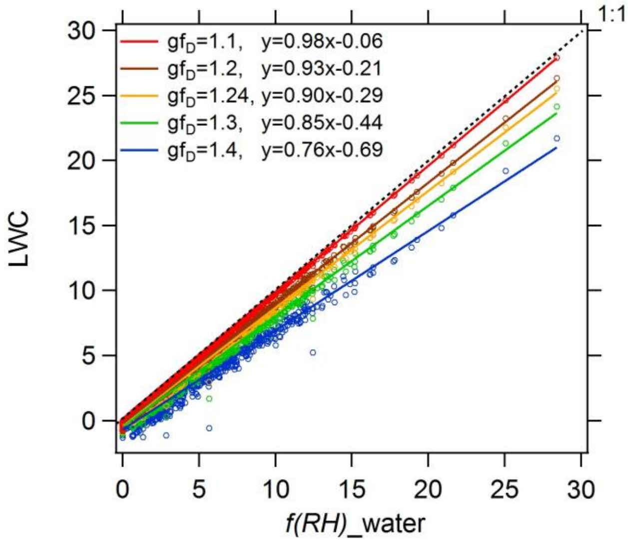

Fig. S5. Comparison between $f(RH)$_water (Eq. 8) and LWC calculated based on $\overline{Q_{s,ambient}}/\overline{Q_{s,dry}}$ at specified gf_D (Eq. 10). Equations from orthogonal regressions are shown.

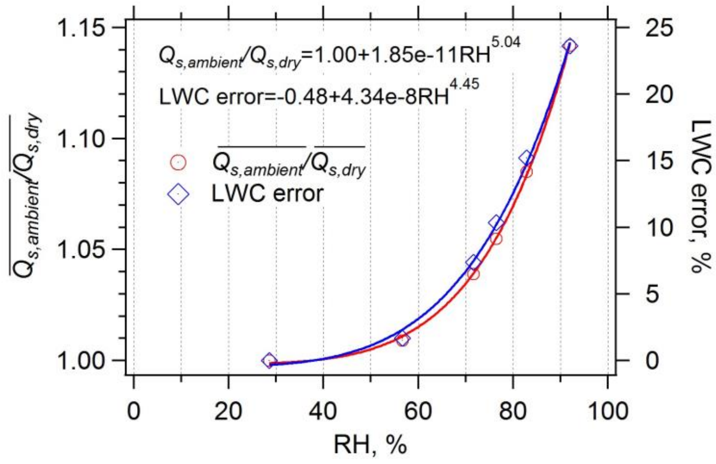

Fig. S6. $\overline{Q_{s,ambient}}/\overline{Q_{s,dry}}$ and LWC error are plotted as a function of RH. The size RH points (28.6%, 56.6%, 71.6%, 76.4%, 82.8%, 92.0%) noted on the graph corresponds to gf_D = 1, 1.1, 1.2, 1.24, 1.3, and 1.4, respectively.

3. Particulate organic hygroscopic parameter, κ_{org}

Overall κ_{org} had a study mean ($\pm$SD) of 0.126 ± 0.059 (Cerully et al., 2014). However, κ_{org} data were not available during the first 20 days of SOAS field study. Therefore, diurnal hourly average κ_{org} was calculated and median values are plotted in Fig. S7. Because κ_{org} median averages were scattered, 3-hr running averages were used to calculate W_o.

The uncertainty of κ at 0.4% supersaturation, which was used to determine the values of κ_{org} (representative of SOAS ambient particles), was 0.033, mentioned in Section 3.2.1 in Cerully et al. (2014). Thus, dividing the absolute uncertainty of 0.033 by the mean κ_{org} gives a relative κ_{org} uncertainty of 26%.

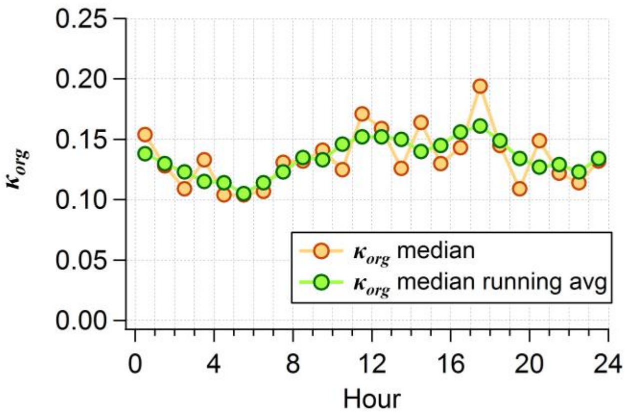

Fig. S7. κ_{org} diurnal variation. Median averages are plotted at local hours.

4. Filter based IC analysis at all sites

High-volume $PM_{2.5}$ filters, sampled in parallel to the AMS measurement, were analyzed by a DIONEX IC (UTAC-ULP1 concentrator column, AG11 guard column and AS11 anion column) to provide chemical information of the refractory ions (Na^+, K^+, Mg^{2+}, Ca^{2+}, PO_4^{3-}). Filter-based nitrate is excluded due to potential artifacts (Hering and Cass, 1999; Chang et al., 2000). The $PM_{2.5}$ inorganic compositions at various sites were similar, all dominated by SO_4 (64-74%) and NH_4^+ (22-31%). We found that less than 5% of the total $PM_{2.5}$ inorganic mass was refractory ions, except RS had the highest fraction as 9%.

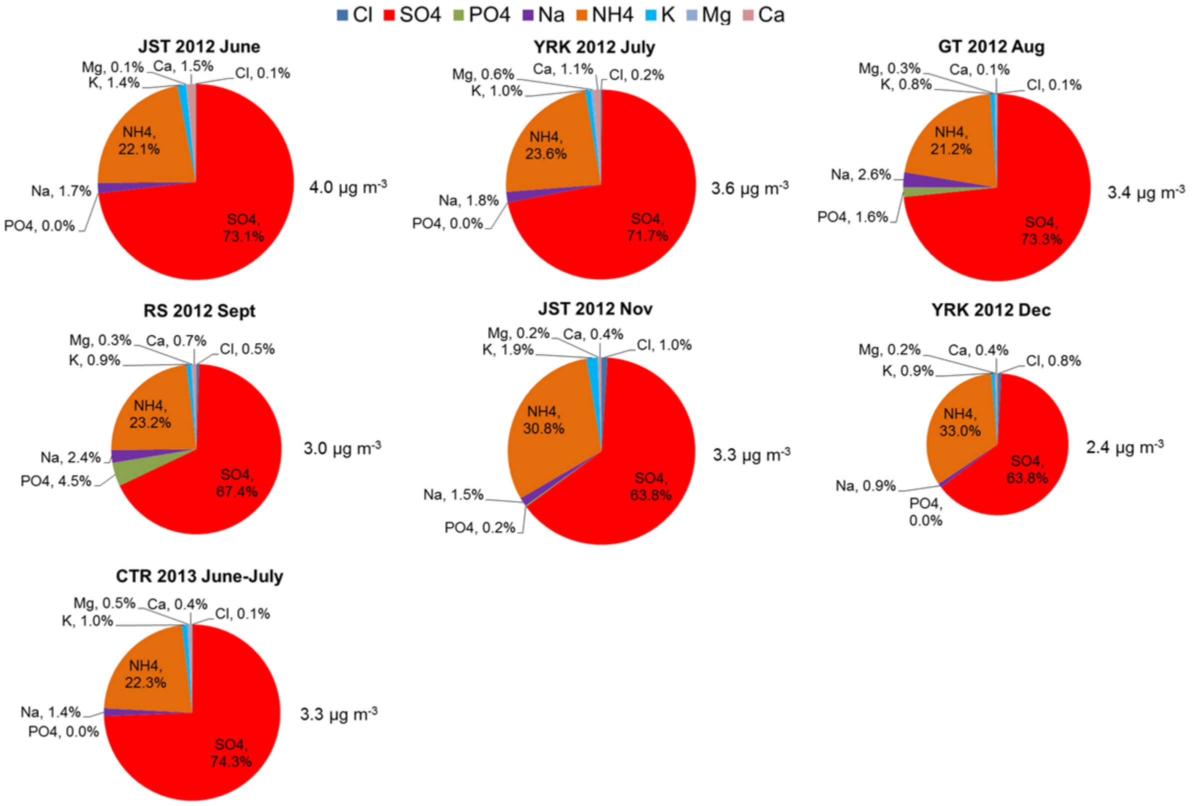

Fig. S8. Filter-based campaign averaged inorganic composition in $PM_{2.5}$ at all sites. The mean concentrations of all the listed ions are labeled to the right of PI charts. Filter sampling, each 23hrs, was parallel to AMS measurement. JST 2012 June is plotted rather than 2012 May due to lack of filter data in 2012 May.

References:

Bergin, M. H., Cass, G. R., Xu, J., Fang, C., Zeng, L. M., Yu, T., Salmon, L. G., Kiang, C. S., Tang, X. Y., Zhang, Y. H., and Chameides, W. L.: Aerosol radiative, physical, and chemical properties in Beijing during June 1999, Journal of Geophysical Research, 106, 17969, 10.1029/2001jd900073, 2001.

Cerully, K. M., Bougiatioti, A., Hite Jr, J. R., Guo, H., Xu, L., Ng, N. L., Weber, R., and Nenes, A.: On the link between hygroscopicity, volatility, and oxidation state of ambient and water-soluble aerosol in the Southeastern United States, Atmospheric Chemistry and Physics Discussions, 14, 30835-30877, 10.5194/acpd-14-30835-2014, 2014.

Chang, M. C., Sioutas, C., Kim, S., Gong, H., and Linn, W. S.: Reduction of nitrate losses from filter and impactor samplers by means of concentration enrichment, Atmospheric Environment, 34, 85-98, Doi 10.1016/S1352-2310(99)00308-8, 2000.

Engelhart, G. J., Asa-Awuku, A., Nenes, A., and Pandis, S. N.: CCN activity and droplet growth kinetics of fresh and aged monoterpene secondary organic aerosol, Atmospheric Chemistry and Physics, 8, 3937-3949, 2008.

Graaff, R., Aarnoudse, J. G., Zijp, J. R., Sloot, P. M. A., de Mul, F. F. M., Greve, J., and Koelink, M. H.: Reduced light-scattering properties for mixtures of spherical particles: a simple approximation derived from Mie calculations, Appl. Opt., 31, 1370-1376, 10.1364/AO.31.001370, 1992.

Greenspan, L.: Humdity Fixed Points of Binary Saturated Aqueous Solutions, Journal of Research of the National Bureau of Standards, 81A, 8, 1977.

Hand, J. L., and Kreidenweis, S. M.: A New Method for Retrieving Particle Refractive Index and Effective Density from Aerosol Size Distribution Data, Aerosol Science and Technology, 36, 1012-1026, 10.1080/02786820290092276, 2002.

Hering, S., and Cass, G.: The Magnitude of Bias in the Measurement of $PM_{2.5}$ Arising from Volatilization of Particulate Nitrate from Teflon Filters, Journal of the Air & Waste Management Association, 49, 725-733, 10.1080/10473289.1999.10463843, 1999.

King, S. M., Rosenoern, T., Shilling, J. E., Chen, Q., and Martin, S. T.: Cloud condensation nucleus activity of secondary organic aerosol particles mixed with sulfate, Geophysical Research Letters, 34, L24806, 10.1029/2007gl030390, 2007.

Kuwata, M., Zorn, S. R., and Martin, S. T.: Using elemental ratios to predict the density of organic material composed of carbon, hydrogen, and oxygen, Environmental science & technology, 46, 787-794, 10.1021/es202525q, 2012.

Laven, P.: MiePlot: a computer program for scattering of light from a sphere using Mie theory & the Debye series, accessed January, 2013.

Nguyen, T. K. V., Petters, M. D., Suda, S. R., Guo, H., Weber, R. J., and Carlton, A. G.: Trends in particle-phase liquid water during the Southern Oxidant and Aerosol Study, Atmospheric Chemistry and Physics, 14, 10911-10930, 10.5194/acp-14-10911-2014, 2014.

Seinfeld, J. H., and Pandis, S. N.: Atmospheric Chemistry and Physics: from Air Pollution to Climate Change 2nd Edition, John Wiley & Sons, Inc., Hoboken, New Jersey, 2006.

Sloane, C. S., Watson, J., Chow, J., Pritchett, L., and Richards, L. W.: Size-Segregated Fine Particle Measurements by Chemical-Species and Their Impact on Visibility Impairment in Denver, Atmospheric Environment. Part A. General Topics, 25, 1013-1024, Doi 10.1016/0960-1686(91)90143-U, 1991.

Stein, S. W., Turpin, B. J., Cai, X. P., Huang, C. P. F., and Mcmurry, P. H.: Measurements of Relative Humidity-Dependent Bounce and Density for Atmospheric Particles Using the DMA-Impactor Technique, Atmospheric Environment, 28, 1739-1746, Doi 10.1016/1352-2310(94)90136-8, 1994.

Stelson, A. W.: Urban aerosol refractive index prediction by partial molar refraction approach, Environmental science & technology, 24, 1676-1679, 1990.

Turpin, B. J., and Lim, H.-J.: Species Contributions to PM2.5 Mass Concentrations: Revisiting Common Assumptions for Estimating Organic Mass, Aerosol Science and Technology, 35, 602-610, 10.1080/02786820119445, 2001.

Wiscombe, W. J.: Improved Mie scattering algorithms, Appl Opt, 19, 1505-1509, 10.1364/AO.19.001505, 1980.